

Liquid amine–solid carbamic acid phase-separation system for direct capture of CO₂ from air

Corresponding author

Prof. Seiji Yamazoe

Department of Chemistry, Graduate School of Science, Tokyo Metropolitan University,
1-1 Minami-Osawa, Hachioji, Tokyo 192-0397, Japan

E-mail address: yamazoe@tmu.ac.jp

List of authors

Soichi Kikkawa^{a,b,c}, Kazushi Amamoto^a, Yu Fujiki^a, Jun Hirayama^{a,b}, Gen Kato^d, Hiroki Miura^{b,c,d}, Tetsuya Shishido^{b,c,d}, and Seiji Yamazoe^{a,b,c,e*}

Affiliations and full postal addresses

- a. Department of Chemistry, Graduate School of Science, Tokyo Metropolitan University, 1-1 Minami-Osawa, Hachioji, Tokyo, 192–0397, Japan
- b. Elements Strategy Initiative for Catalysts & Batteries (ESICB), Kyoto University, 1-30 Goryo-Ohara, Nishikyo-ku, Kyoto, 615–8245, Japan
- c. Research Center for Hydrogen Energy-Based Society, Tokyo Metropolitan University, 1-1 Minami-Osawa, Hachioji, Tokyo 192–0397, Japan
- d. Department of Applied Chemistry for Environment, Graduate School of Urban Environmental Sciences, Tokyo Metropolitan University, 1-1 Minami-Osawa, Hachioji, Tokyo, 192–0397, Japan
- e. Precursory Research for Embryonic Science and Technology (PRESTO), Japan Science and Technology Agency (JST), 4-1-8, Honcho, Kawaguchi-shi, Saitama 332-0012, Japan

Abstract

The phase separation between a liquid amine and the solid carbamic acid exhibited >99% CO₂ removal efficiency under a large-scale gas stream of 400 ppm CO₂. Isophorone diamine [IPDA; 3-(aminomethyl)-3,5,5-trimethylcyclohexylamine] reacted with CO₂ in the CO₂/IPDA molar ratio of ≥ 1 even in H₂O as a solvent. The captured CO₂ was completely desorbed at 333 K because the dissolved carbamate ion releases CO₂ at low temperature. The reusability of IPDA under CO₂ adsorption-and-desorption cycles without degradation, the >95% efficiency kept for 100 hours under direct air capture condition, and high CO₂ capture rate (214 mmol/h for 1 mol amine) suggest that the phase separation system using IPDA is robust and durable for practical use.

Introduction

Reducing the concentration of carbon dioxide (CO₂) in the atmosphere is becoming essential for building a sustainable society because an increase in the atmospheric concentration of CO₂ is closely linked to global warming and climate change.¹ Reduction of atmospheric CO₂ levels will require a concerted effort to both limit future emissions of CO₂ and to implement strategies for decreasing the existing atmospheric concentration of CO₂. Artificial storage of CO₂ through direct injection into underground strata or the oceans is relatively well established and has attained plant-level operation;^{2, 3} however, such carbon capture and storage techniques involve the risk of subsequent CO₂ leakage. On the other hand, the utilization of CO₂ as a value-added product by carbon capture and storage (CCS) is expected to provide a potential strategy for maintaining net CO₂ emissions at zero.⁴⁻⁷ However, the existing CCS technology

requires further development to improve the CO₂ absorption/desorption efficiency of sorbents and to establish methods for subsequent conversion of captured CO₂.

Among CCS techniques, the sorbents for capturing atmospheric <500 ppm of CO₂ without any condensation and separation, known as direct air capture (DAC), is a promising technology and desired to operate under a large stream of ambient or low-pressure compressed gas.⁷⁻⁹ The challenges in the sorbents for DAC techniques is high absorption efficiency of low-concentration CO₂, because the existing CCS techniques have insufficient absorption efficiency to perfectly remove the low-concentration CO₂. In addition, the desorption of the adsorbed CO₂ should require as little energy as possible; currently, the most-well-established sorbent, 2-aminoethanol (monoethanolamine; MEA), requires a temperature of >473 K for efficient desorption.^{6, 10-12} Finally, the reusability and durability of the sorbents for use in CO₂ capture-and-desorption cycles is required to reduce the frequency of their regeneration and/or replacement. An ideal sorbent should be easily separated and collected from the absorption apparatus for subsequent regeneration.

To satisfy these demands, a number of solid amine-based sorbents¹³⁻¹⁹ and CO₂-absorption systems that utilize phase separation²⁰⁻²⁷ have been developed. The ability of homogeneous liquid-phase systems to absorb CO₂ has been improved by modifying the structures of the amine sorbents. For example, Inagaki *et al.* reported that the introduction of the hydrophobic phenyl group into alkylamines enhances their CO₂-absorption ability through the formation of a liquid bilayer structure.²⁸ Hanusch *et al.* discovered that pyrrolizidine-based diamines showed more-efficient CO₂ capture than does conventional MEA (**Fig. 1A-a**).²⁹ Although these are promising sorbents for CO₂ capture and desorption, further improvements in the rate of CO₂ absorption and more efficient

absorption at low CO₂ concentrations are required. Liquid–liquid phase-separation of amine–H₂O mixtures with lower critical solution temperatures have recently been developed to reduce the costs of regenerating the sorbent (**Fig. 1A-b**).^{23, 30, 31} After CO₂ absorption, the organic and aqueous phases in these phase-change systems are immiscible, of which CO₂-rich aqueous phase are suitable to concentrate CO₂ by heating.²³ Such systems have achieved higher CO₂ capacities and lower costs compared with those of conventional MEA sorbent-based systems.³⁰ However, the solvents used in the phase-change systems are volatile and corrosive, limiting their range of operating conditions. Actually, the abovementioned systems were evaluated in static systems under ambient or high-pressure CO₂. To establish an efficient system for the large-scale streams of low-concentration CO₂, new concepts for sorbents are required.

According to the proposed carbamate mechanism of MEA [$2R^1R^2NH(l) + CO_2(g) \rightarrow R^1R^2NCOO^-(l) + R^1R^2NH_2^+(l)$], the produced carbamate ion inhibits the forward reaction.³² Liquid–solid phase separation provides a possible way of overcoming the equilibrium limitations that inhibits the efficient CO₂ absorption. If the products from the absorption of CO₂ are solids, their equilibrium concentration in the liquid phase will remain low, thus leading high absorption rate of CO₂ into the liquid phase. Moreover, as another benefit, liquid sorbents contact dissolved CO₂ much more efficiently than do solid sorbents, which allow efficient absorption of low-concentration CO₂ from large-scale gas streams. Same liquid–solid phase separation systems have been reported up to now under high concentrated CO₂ conditions using potassium proline,²⁶ bis(iminoguanidine),²⁴ and triethylenetetramine with polyethylene glycol.²² A DAC system using liquid–solid phase separation with an iminoguanidine-based sorbent for CO₂ has recently been reported (**Fig. 1A-c**).²⁵ Although CO₂ desorption from the CO₂-incorporated crystal

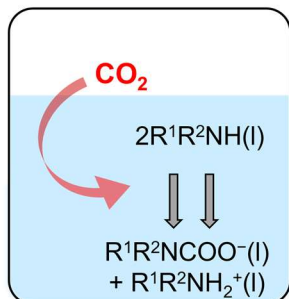
began at 333 K, complete CO₂ release required high temperatures above 393 K. In addition, this system requires a large amount of solvent because of low solubility of the sorbent. Custelcean *et al.* recently developed DAC system using amino acid potassium solution followed by the reaction with guanidine compound resulting in crystallization of insoluble carbonate salt.^{20, 21} These systems could remove CO₂ from air, but the system requires sequential CO₂ transfer system. Further research is therefore required to develop a versatile and simple solid–liquid separation system that are suitable for ambient CO₂ absorption and that lead efficient CO₂ desorption at low temperatures.

Here, we focus on carbamic acids that exist as a minor-route intermediates $[R^1R^2NH(l) + CO_2(g) \rightarrow R^1R^2NCOOH(l)]$.^{32, 33} Especially, the carbamic acids that have low solubility compared with corresponding liquid amines are promising to solidification. If a liquid amine forms a solid carbamic acid by reaction with CO₂ $[R^1R^2NH(l) + CO_2(g) \rightarrow R^1R^2NCOOH(s)]$, an efficient CO₂ absorption system might be established due to the liquid–solid phase separation and the high amine-utilization efficiency (a 1:1 CO₂-to-amine ratio) (**Fig. 1A-d**). Especially, this liquid–solid phase change with carbamic acid formation would lead high absorption rate of CO₂ even at a low CO₂ concentration and large stream, which could not be achieved by using the existing CO₂ absorption systems. Furthermore, in the desorption system under heating, the increase in solubility of solid carbamic acids would aid the efficient desorption of CO₂.

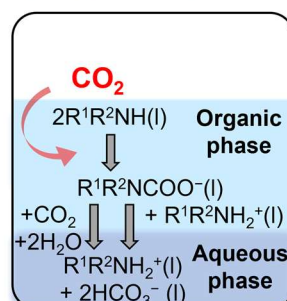
We investigated a number of amine compounds to prove our hypothesis. First, we evaluated their CO₂ removal efficiency in a flow system under a large stream of ambient CO₂ (**Fig. 1B**). We found that cyclohexyldiamines showed the best properties as liquid–solid phase-separation sorbents. In particular, isophorone diamine [IPDA; 3-(aminomethyl)-3,5,5-trimethylcyclohexylamine] exhibited a superior CO₂ absorption

efficiency under a wide range of CO₂ concentrations (400 ppm to 30%) in a N₂ stream, with solidification of the corresponding carbamic acid. The highly efficient CO₂ removal liquid–solid phase-separation phenomenon was observed in various solvents including H₂O. Moreover, this carbamic acid discharged CO₂ at a lower temperature than a conventional MEA-based system and it exhibited remarkable reusability. This benchmark study is the first demonstration of a potential large-stream DAC system with >90% CO₂ removal efficiency and reusability that is based on the phase separation between a liquid amine sorbent and a solid carbamic acid.

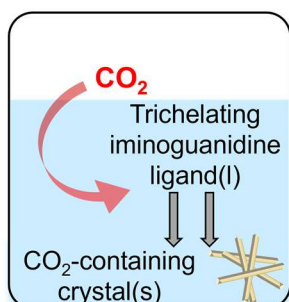
(A-a)
A typical carbamate mechanism
(single phase)



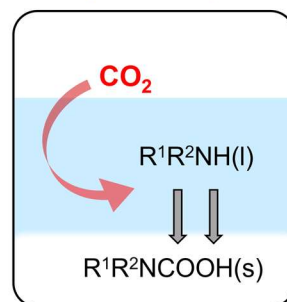
(A-b)
Immiscible organic–aqueous
liquid-phase separation



(A-c)
Phase separation between liquid
amine and CO_2 -containing crystal



(A-d)
Phase separation between liquid
amine and solid carbamic acid
(This work)



(B)

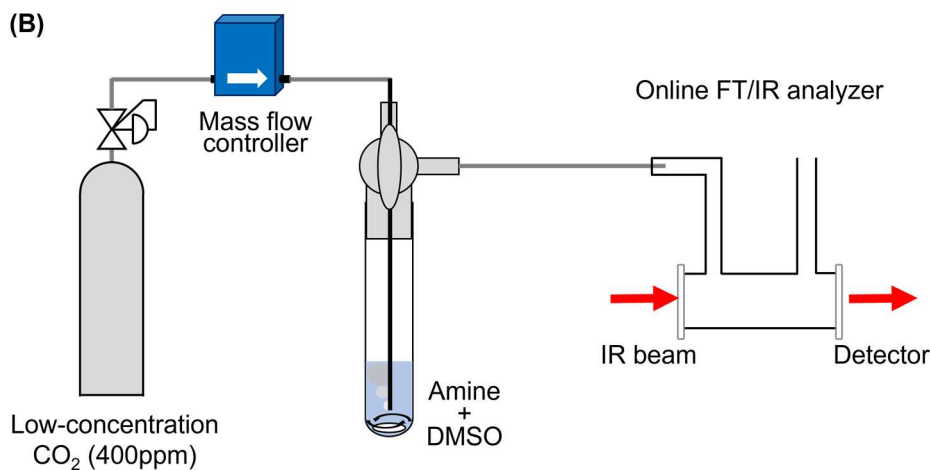


Fig. 1(A) CO_2 absorption/desorption system using phase separation. (a) a typical carbamate mechanism (Ref. 32). (b) Liquid–liquid phase-change solvents (Ref. 23). (c) Liquid–solid phase separation with an iminoguanidine-based sorbent (Ref. 25). (d) Liquid–solid phase separation with solid carbamate acid formation (This work). **(B)** An ambient-flow-type reactor equipped with online FT/IR analyzer for direct air capture system.

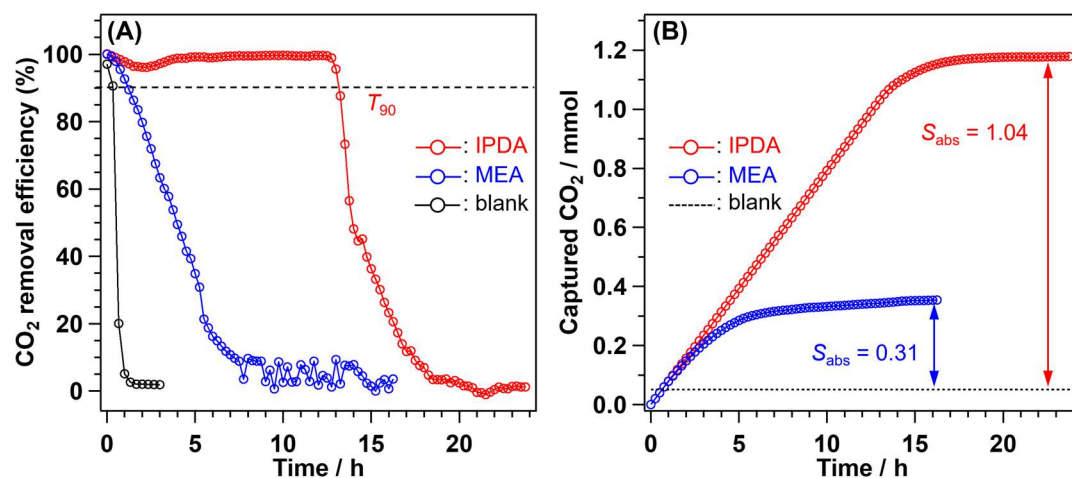


Fig. 2. (A) CO₂ removal efficiency over IPDA (red circles) and MEA (blue circles). Black circles represent the downstream CO₂ concentration w/o amine. (B) Total amounts of captured CO₂ over IPDA (red circles) and MEA (blue circles). Dashed line represents the amount of captured CO₂ in DMSO. 400ppm CO₂–N₂ at a flow rate of 75 mL min⁻¹. Amines: 1 mmol, DMSO: 1 mL.

Fig. 2A shows the efficiency of removal of 400 ppm of CO₂ from a flowing CO₂–N₂ mixture for amine-based sorbents in dimethyl sulfoxide (DMSO) solution, respectively. IPDA maintained almost a 100% efficiency (CO₂ absorption rate: 80 mmol h⁻¹ for 1 mol amine) for CO₂ removal over 12 hours; its efficiency then suddenly decreased, reaching 0% after 21 hours. The total amount of captured CO₂ (S_{abs}) by IPDA reached 1.04 mmol (**Fig. 2B** and **Supplementary Table 1**). **Fig. 3** and **Supporting Information Video S1** show the changes that occurred during the CO₂ absorption process of **Fig. 2**. A white solid formed after a reaction time of 2.5 hours, and the viscosity of IPDA solution gradually increased as the formation of the precipitate. MEA, a typical amine-based sorbent, showed a lower efficiency of CO₂ removal than IPDA under the same conditions (**Fig. 2A**). After 10 hours, the removal efficiency of MEA reached 0% with a S_{abs} of 0.31 mmol. ¹³C NMR spectroscopy revealed that the precipitate consisted

of [3-(aminomethyl)-3,5,5-trimethylcyclohexyl]carbamic acid (**CA1**) (**Supplementary Fig. 1A**). Hanusch *et al.* reported that the solid carbamic acids from aminopyrrolidines (the structures of which were established by means of single-crystal X-ray diffraction) formed through intramolecular or intermolecular cooperative activation of their primary and tertiary amino groups.²⁹ IPDA also formed **CA1** by interaction of its amino groups with CO₂.

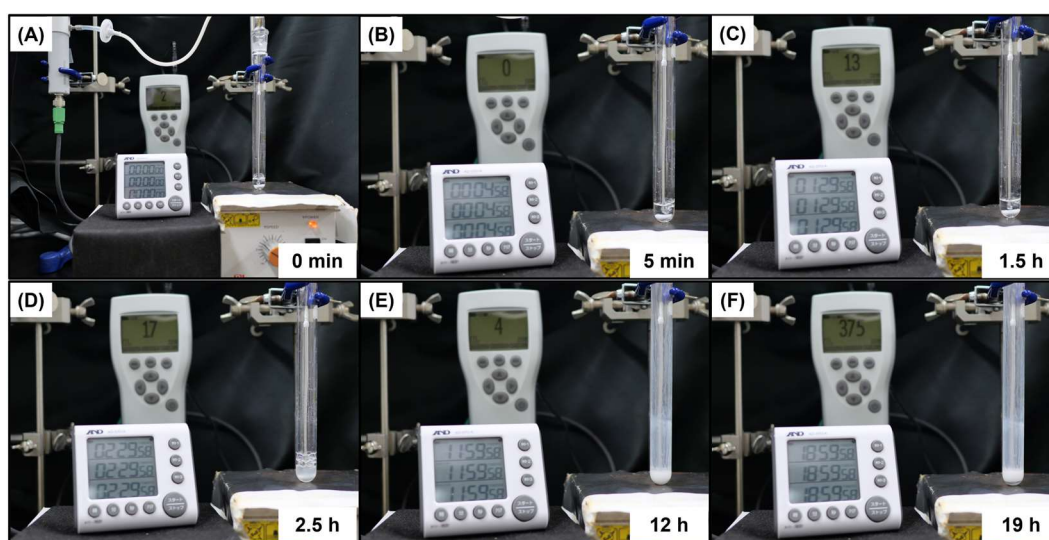


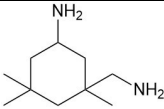
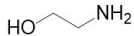
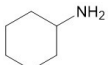
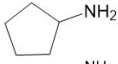
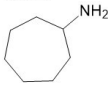
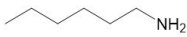
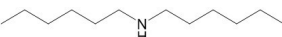
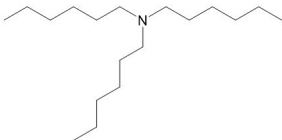
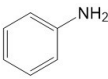
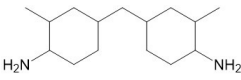
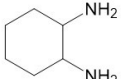
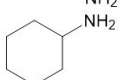
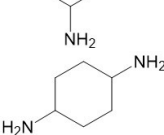
Fig. 3. Photographs of a DMSO solution of IPDA under a 400 ppm CO₂–N₂ flow. (A) 0 min, (B) 5 min, (C) 1.5 h, (D) 2.5 h, (E) 12 h, and (F) 19 h. The downstream concentration CO₂ was monitored by using a nondispersive infrared CO₂ meter (GMP252, Vaisala GmbH).

The IPDA also showed higher CO₂ removal efficiencies even under the 1% and 30% CO₂ conditions than MEA as shown in **Supplementary Fig. 2**. In the case of 30% CO₂, the CO₂-removal efficiency over IPDA remained above 90% over 24 min with a S_{abs} of 6.21 mmol. MEA showed a slightly lower durability and capacity ($S_{\text{abs}} = 4.46$ mmol). The S_{abs} /amine molecule ratios ($R_{\text{CO}_2/\text{molecule}}$) for IPDA hardly depended on the CO₂ concentration, whereas those for MEA drastically decreased when using a low

concentration CO₂ (**Supplementary Table 1**). Thus, IPDA is a superior sorbent to MEA over a wide range of CO₂ concentrations.

Next, amine scope has been carried out to determine the suitable amine compound for this liquid–solid phase-separation system. **Table 1** and **Supplementary Fig. 3** summarize the CO₂-absorption capacities of various amines under a 1% CO₂–N₂ flow. IPDA exhibited a superior CO₂ absorption durability even to that of equimolar-amine-containing MEA (Table 1, entries 1–3). $R_{\text{CO}_2/\text{molecule}}$ for cycloalkyl amines (entries 4–6) was <0.6, which was *ca.* half of that of IPDA (entry 1). In addition, the T_{90} of these amines (entries 4–6) were shorter than that of IPDA (entry 1). Primary amines showed superior amine efficiencies to those of secondary and tertiary amines, probably due to steric hindrance (entries 7–9). In addition, aniline, in which the primary amine group is attached to a phenyl group, absorbed hardly any CO₂ (entry 10). Cycloalkyl diamines (entries 1 and 11–14) formed precipitates and showed relatively high T_{90} values. For all the diamines investigated in this study, $R_{\text{CO}_2/\text{molecule}} \approx 1.0$. In addition, IPDA exhibited a CO₂-removal efficiency over a long time ($T_{90} = 121$ min). Among the regioisomeric cyclohexyldiamines (entries 12–14), cyclohexane-1,2-diamine, with a low T_{90} value of 36 min, afforded a less-viscous solution. These results show that the polarity of the carbamic acid is essential for efficient CO₂ removal and that differences in the absorption efficiency arise from the rate of formation and the solubility of precipitates from CO₂-absorption reactions.

Table 1. CO₂ absorption capacities of various amines^a

Entry	Amine	Precipitate	T_{90} / min	R_{CO_2} /molecule
1	IPDA 	formed	121	1.08
2	MEA	n.d.	43	0.62
3	MEA ^b 	n.d.	68	0.60
4	cyclohexylamine 	n.d.	27	0.56
5	cyclopentylamine 	n.d.	23	0.49
6	cycloheptylamine 	n.d.	28	0.53
7	hexylamine 	n.d.	55	0.76
8	dihexylamine 	n.d.	9	0.23
9	triethylamine 	n.d.	6	n.d.
10	aniline 	n.d.	2	n.d.
11	4,4'-methylenebis-(2-methylcyclohexylamine) 	formed	61	1.02
12	cyclohexane-1,2-diamine 	partially formed	36	0.92
13	cyclohexane-1,3-diamine 	formed	104	1.04
14	cyclohexane-1,4-diamine 	formed	64	0.98

^a CO₂ absorption capability was evaluated under 1% CO₂-N₂ flow. Flow rate: 20 mL min⁻¹, Amines: 1 mmol, DMSO: 5 mL.

^b 2 mmol of MEA was applied, which contains equimolar of amino groups to 1 mmol of IPDA.

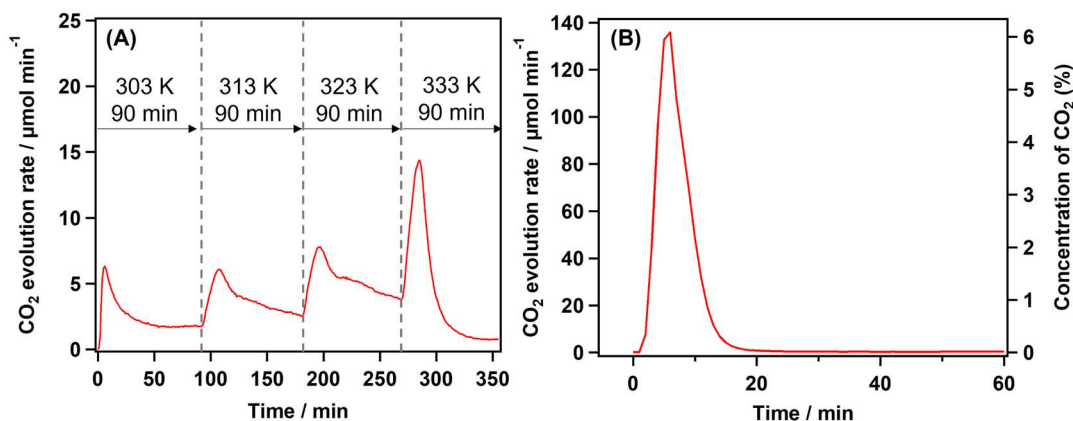


Fig. 4. The desorption profile of CO₂ over 1 mmol of **CA1** in 15 mL of DMSO under N₂ flow (50 mL min⁻¹). **(A)** The solution temperature raised at a range of 303–333 K step-by-step with a 90-min interval. **(B)** The solution was heated at 373 K.

The CO₂-desorption properties of **CA1** were also investigated. **Fig. 4A** shows the desorption rate of CO₂ at various temperatures. CO₂ desorption was first observed at 303 K. Further desorption occurred on increasing the temperature, and the CO₂ was completely desorbed at 333 K. As desorption occurred, the precipitate gradually vanished. **Fig. 4B** shows the desorption profile of CO₂ at 373 K. CO₂ desorption was finished within 20 minutes, and the maximum CO₂-desorption rate was 134 μmol min⁻¹. This indicates the low-concentration CO₂ as ambient air could be condensed to 6% CO₂.

The reusability of IPDA as a sorbent was also examined (**Fig. 5**). The > 90% CO₂-capture efficiency was kept for 120 min and, after switching the gas to N₂ and ramping the temperature to 333 K, the captured CO₂ was perfectly released into the inert gas. The absorption-and-desorption profile is therefore repeatable at least five times without degradation. Note that the desorption temperature was 333 K, which is lower than that for the conventional desorption system with MEA.¹⁰⁻¹² We therefore consider that

IPDA has the potential to replace the existing sorbent in absorption/desorption systems with MEA, requires a temperature of >473 K.^{6, 10-12}

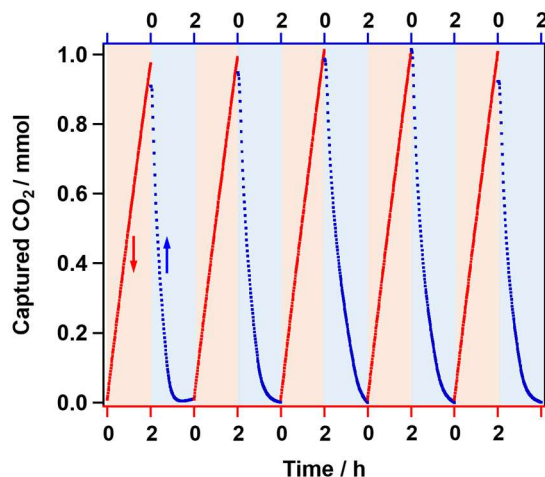


Fig. 5. The repetition profile of CO₂ absorption/desorption over 1 mmol IPDA in 15 mL of DMSO. The absorption capability test under 1% CO₂-N₂ flow (20 mL min⁻¹, 298 K, red line) and desorption of CO₂ under N₂ flow (50 mL min⁻¹, 333 K, blue line) were switched for 5 times with a 120-min interval. The left axis represents the total amounts of captured CO₂.

In this study, we found that IPDA efficiently absorbed CO₂ over a wide range of concentrations ranging from 400 ppm to 30% with $>90\%$ CO₂ removal efficiency in a flow system and the formation of precipitates of a carbamic acid product. This performance is superior to that of a comparable conventional CO₂-absorption system using MEA. The IPDA-based liquid–solid phase separation system has two advantages. The first is its high $R_{\text{CO}_2/\text{molecule}}$ ratio. The $R_{\text{CO}_2/\text{molecule}}$ ratio for a typical CO₂-absorption system involving a carbamate mechanism is about 0.5 [$2\text{R}^1\text{R}^2\text{NH} + \text{CO}_2 \leftrightarrow \text{R}^1\text{R}^2\text{NCOO}^- \cdots \text{R}^1\text{R}^2\text{NH}_2^+$],³² whereas the $R_{\text{CO}_2/\text{molecule}}$ ratio for the IPDA-based carbamic acid system was near 1.0 [$\text{R}^1\text{R}^2\text{NH}(\text{l}) + \text{CO}_2(\text{g}) \leftrightarrow \text{R}^1\text{R}^2\text{NCOOH}(\text{s})$]. The second advantage is the high CO₂ removal efficiency (T_{90} value) of the liquid–solid phase

separation system, which is achieved as follows. The IPDA reacts with CO₂ to form the corresponding carbamic acid in the liquid phase. Initially, the concentrations of carbamic acid in the solution increase to maintain the equilibrium with carbamate ion $[R^1R^2NCOO^- \cdots R^1R^2NH_2^+(l) \leftrightarrow R^1R^2NH(l) + R^1R^2NCOOH(l)]$.³² When its concentration is saturated, the carbamic acid precipitates from the solution $[R^1R^2NCOOH(l) \leftrightarrow R^1R^2NCOOH(s)]$. In fact, the white carbamate-acid precipitate formed after a reaction time of 1.5 hours, as shown in **Fig. 3** and **Supporting Information Video 1**. In addition, the T_{90} strongly depended on the amine concentration and a highly concentrated solution of IPDA showed a high T_{90} value with a high space velocity (SV; flow rate/volume of solution) of 240 h⁻¹ (see **Supplementary Fig. 4A** and **Supplementary Table 2**). The high CO₂ removal efficiency was also achieved at high IPDA concentration condition (1 mmol IPDA/1 mL DMSO, **Fig. 2A**) at SV of 4500 h⁻¹. In the case of cyclohexylamine which does not form a carbamic acid precipitate, the CO₂ absorption behaviour was independent of the amine concentration (DMSO: 5–15 mL, SV = 80–240 h⁻¹) whereas 1 mmol cyclohexylamine in 1 mL of DMSO showed 90% CO₂ removal efficiency under 1% CO₂ condition with the formation of precipitate, which was confirmed by ¹³C NMR spectroscopy (**Supplementary Fig. 1B** and **Supplementary Fig. 4B**). These results indicate that a high concentration of IPDA favours CO₂ absorption and the maintenance of a high absorption rate due to the ease with which solution becomes saturated with liquid carbamic acid, resulting in continuous formation of the carbamic acid precipitate (**Fig. 6A**). The phase-separation system therefore overcomes the limitations imposed by the carbamate-ion concentration and the $R_{CO_2/molecule}$ ratio. Inagaki *et al.* reported that phenyl group-containing alkylamines, such as 1,3-phenylenedimethanamine and phenylmethanamine exhibited efficient CO₂ capacity for DAC system.²⁸ We also tested

those amines and found 1,3-phenylenedimethanamine showed a comparable CO₂ removal efficiency (T_{90}) and CO₂ absorption capacity to IPDA (**Supplementary Fig. 5**). This diamine formed precipitates when absorbing CO₂, whereas phenylmethanamine maintained the liquid form with showing low CO₂ removal efficiency. We conclude that phase separation between the liquid amine and the solid carbamic acid allows a high amine-utilization efficiency and a high CO₂-removal efficiency compared with conventional MEA solution, even at ambient CO₂ concentrations.

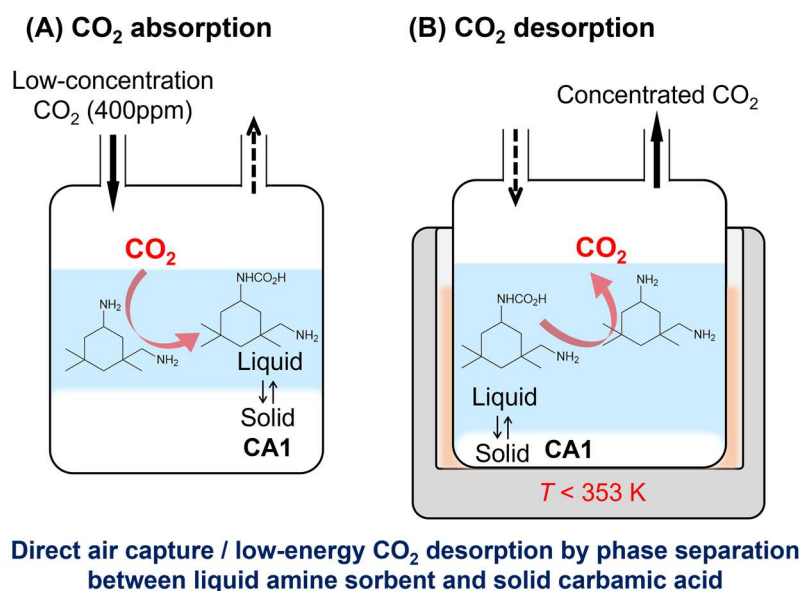


Fig. 6. Schematic image of CO₂ (A) absorption and (B) desorption system using phase separation between liquid IPDA and solid CA1.

We also found that CO₂ evolution from the CO₂-absorbed solution containing solid CA1 began to occur at 303 K under a gas flow and that 6% concentration of CO₂ was achieved at 373 K. Thermogravimetry/mass (TG-MS) profile of the solid CA1 showed two steps of weight losses (**Supplementary Fig. 6**); the first step, which occurred above 333 K, was accompanied with the desorption of CO₂ ($m/z = 44$), and the second

step, above 383 K, was attributed to volatilization of IPDA, as its fragmentation patterns appeared in the mass spectrum. Therefore, **CA1** should desorb CO₂ without volatilization in the temperature range 333–383 K. However, the desorption of CO₂ from the CO₂-absorbed solution occurred at a lower temperature than that required for solid **CA1**. This suggests that a part of carbamic acid is dissolved in solution and the carbamic ion, which is formed from carbamic acid in solution, desorb CO₂ at a low temperature. In addition, the concentration of liquid carbamic acid and carbamate ion increased on heating the solution because the solubility of **CA1** increases with increasing temperature (**Fig. 6B**). The liquid–solid phase-separation system is therefore also suitable for the CO₂-desorption process.

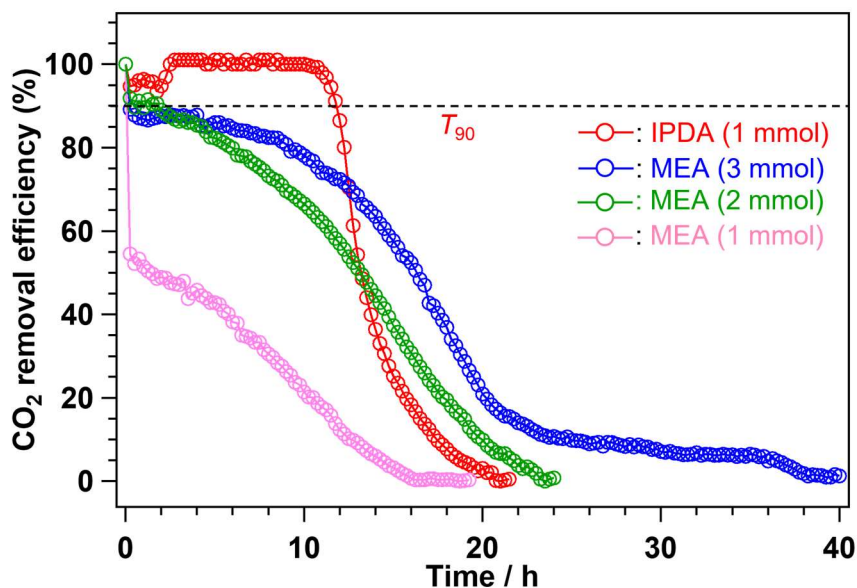


Fig. 7. CO₂ removal efficiency over 1 mmol of IPDA (red circles) and MEA (3 mmol, blue circles; 2 mmol; green circles, 1mmol; pink circles). 400ppm CO₂–N₂ at a flow rate of 75 mL min^{−1}. H₂O: 1 mL.

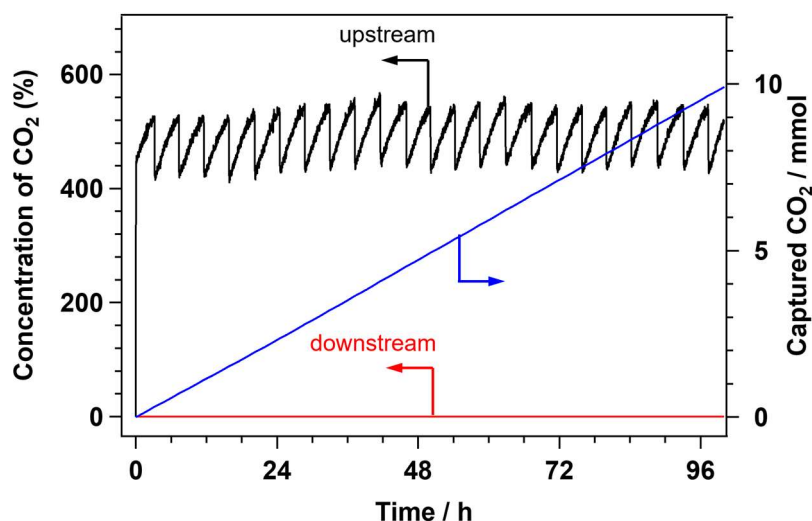


Fig. 8. CO₂ concentration at a downstream (red line) and upstream (black line) of the reactor under a compressed ambient air. Total amount of absorbed CO₂ is represented in a right axis. IPDA: 20 mmol, H₂O: 50 mL, gas flow rate: 75 mL min⁻¹. The CO₂ concentration was monitored by using a nondispersive infrared CO₂ meter (GMP252, Vaisala GmbH).

Among the diamine-based sorbents tested in this study, IPDA exhibited the best performance that would be relating to the solubility and thermal stability of solid carbamic acid (**Supplementary Table 3**). Carbamic acids from aminopyrrolidines have been reported as being formed by cooperative activation of their primary and tertiary amino groups, either intramolecularly or intermolecularly.²⁹ The intramolecular arrangement of the amino groups of IPDA should result in efficiency in both the formation of the solid precipitate and the reverse reaction. Compared with the reported liquid–solid pair of insoluble carbonate crystals,²⁵ the high solubility of IPDA in DMSO leads a higher density of captured CO₂ than that of chelate-ligating iminoguanidine, which has a low solubility. Moreover, the strong hydrogen-bonding network between the iminoguanidinium cation and the bicarbonate anion required a desorption energy of 81 kJ mol_{CO₂}⁻¹ and heating to >393 K.²⁵ The Gibbs free energy for the carbamation reaction

has been reported to be $>40 \text{ kJ mol}_{\text{CO}_2}^{-1}$ for a series of primary and secondary amines,³⁴⁻³⁶ which is close to that of the present system. Consequently, CO_2 desorption in the liquid amine–solid carbamic acid phase-separation system proceeds at a low temperature.

Finally, to prove the general versatility of this liquid–solid phase-separation system, solvent effect on the CO_2 removal efficiency was tested as shown in **Supplementary Fig. 7**. The precipitate formed when either DMSO, *N,N*-dimethylformamide (DMF), H_2O , or toluene was used as the solvent at an amine-to-solvent ratio of 1 mmol per 5 mL, whereas the liquid form was maintained for a long time when using methanol as a solvent, suggesting that the production of a precipitate upon CO_2 storage is governed by the solubility of the carbamic acid in each solvent (**Supplementary Table 3**). The IPDA exhibited higher absorption efficiency as compared to MEA with equivalent molar amount (1 mmol MEA), amino groups (2 mmol MEA) and weight (3 mmol MEA) in H_2O solvent (**Fig. 7**). Moreover, CO_2 absorption rate increased after 3 h accompanied with the formation of solid **CA1**. Even at high space velocity, CO_2 absorption rate was enhanced after the **CA1** formation, achieving 214 mmol h^{-1} for 1 mol amine with $>90\%$ CO_2 removal efficiency at $\text{SV} = 6000 \text{ h}^{-1}$ (**Supplementary Fig. 8**). Moreover, IPDA maintained the $>99\%$ removal efficiency of ambient CO_2 from air for 100 hours with the wide-range supply rate of CO_2 ($83\text{--}114 \mu\text{mol h}^{-1}$) (**Fig. 8**). Recently, some efficient amines for DAC, such as 1,3-phenylenedimethanamine (CO_2 absorption rate: 32 mmol h^{-1} for 1 mol amine)²⁸ and pyrrolizidine (CO_2 absorption rate: 5.0 mmol h^{-1} for 1 mol amine)²⁹ were reported (**Supplementary Table 4**). In the DAC system using amino acid potassium and guanidine, the CO_2 absorption rate was reported to be *ca* 95 mmol h^{-1} for 1 mol amine.^{20, 21} The DAC system using alkaline base solution has been established in a plant-level operation with

the CO₂ absorption rate of 16 mmol h⁻¹ for 1 mol NaOH³⁷ and 13 mmol h⁻¹ for 1 mol KOH,³⁸ however, the CO₂ desorption temperature is 1173 K,^{7, 38-41} which is extremely higher than the CO₂ desorption temperature of the present system (333 K). Those results suggest that IPDA, which absorbs CO₂ with sufficient rapidity (CO₂ absorption rate: 214 mmol h⁻¹ for 1 mol amine, SV: 6000 h⁻¹, **Supplementary Fig. 8**), might be a potential candidate for use as an amine-based sorbent for low concentrations of CO₂ and should be suitable for use in a DAC system. In addition, the system works well in H₂O solvent, promising to steam condense the absorbed CO₂ using steam-assisted temperature vacuum-swing adsorption technique.^{42, 43} Those features realize high CO₂ absorption and desorption abilities, and our study has demonstrated the possibility of practical applications in low-energy DAC and CO₂-desorption systems.

Conclusion

In this study, we have developed a system for capturing CO₂ directly from air by using the phase separation between a liquid amine and the solid carbamic acid formed through the absorption of CO₂ by the amine. IPDA exhibited a CO₂ removal efficiency superior to that of conventional MEA for a wide range of CO₂ concentrations (400 ppm to 30%). Remarkably, under a large-scale gas stream containing 400 ppm of CO₂, IPDA reacted with CO₂ in the CO₂/IPDA molar ratio of ≥ 1 and exhibited >99% CO₂ removal over 12 hours, even in H₂O as a solvent, suggesting that it is a suitable sorbent for use in a direct air capture system. The IPDA system began to desorb CO₂ at ≥ 303 K and CO₂ was completely desorbed at 333 K under N₂ flow condition. The CO₂ capture-and-desorption cycle could be repeated at least five times without degradation, proving that IPDA is sufficiently robust and durable for practical use. The removal of IPDA-derived

carbamic acid from the liquid phase as solid during CO₂ absorption realizes high CO₂ removal efficiency even at the large-scale gas stream (space velocity: 6000 h⁻¹ and CO₂ supply rate: 214 mmol h⁻¹ for 1 mol IPDA) at low CO₂ condition (400 ppm). Moreover, the partially-dissolved IPDA-derived carbamic acid easily releases CO₂ in the liquid phase at low temperature during the CO₂ desorption process. This phase separation system between a liquid amine and the solid carbamic acid formed through absorption/desorption of CO₂ is available for other amines which form solid carbamic acid by CO₂ absorption. Therefore, the solidification of the sorbent should aid in efficient CO₂ absorption compared with the typical carbamate-based mechanism of the conventional MEA-based system.

References

1. R. K. Pachauri, M. R. Allen, V. R. Barros, J. Broome, W. Cramer, R. Christ, J. A. Church, L. Clarke, Q. Dahe and P. Dasgupta, *Climate Change 2014: Synthesis Report. Contribution of Working Groups I, II and III to the Fifth Assessment Report of the Intergovernmental Panel on Climate Change*, IPCC, 2014.
2. E. I. Koytsoumpa, C. Bergins and E. Kakaras, *The Journal of Supercritical Fluids*, 2018, **132**, 3–16.
3. Y. Tanaka, Y. Sawada, D. Tanase, J. Tanaka, S. Shiomi and T. Kasukawa, *Energy Procedia*, 2017, **114**, 5836–5846.
4. H. Yang, Z. Xu, M. Fan, R. Gupta, R. B. Slimane, A. E. Bland and I. Wright, *J. Environ. Sci.*, 2008, **20**, 14–27.
5. M. Mikkelsen, M. Jørgensen and F. C. Krebs, *Energy Environ. Sci.*, 2010, **3**, 43–81.
6. R. M. Cuéllar-Franca and A. Azapagic, *J. CO₂ Util.*, 2015, **9**, 82–102.
7. E. S. Sanz-Perez, C. R. Murdock, S. A. Didas and C. W. Jones, *Chem. Rev.*, 2016, **116**, 11840–11876.
8. R. Socolow, M. Desmond, R. Aines, J. Blackstock, O. Bolland, T. Kaarsberg, N. Lewis, M. Mazzotti, A. Pfeffer and K. Sawyer, *Direct air capture of CO₂ with chemicals: A technology assessment for the APS Panel on Public Affairs*, American Physical Society,

- 2011.
9. A. Goeppert, M. Czaun, G. S. Prakash and G. A. Olah, *Energy Environ. Sci.*, 2012, **5**, 7833–7853.
10. P. Luis, *Desalination*, 2016, **380**, 93–99.
11. M. Wang, M. Wang, N. Rao, J. Li and J. Li, *RSC Advances*, 2018, **8**, 1987–1992.
12. Y. Liu, W. Fan, K. Wang and J. Wang, *J. Clean. Prod.*, 2016, **112**, 4012–4021.
13. E. E. Ünveren, B. Ö. Monkul, Ş. Sarioğlu, N. Karademir and E. Alper, *Petroleum*, 2017, **3**, 37–50.
14. J. Wang, M. Wang, W. Li, W. Qiao, D. Long and L. Ling, *AIChE*, 2015, **61**, 972–980.
15. K. Min, W. Choi, C. Kim and M. Choi, *Nat. Commun.*, 2018, **9**, 726–732.
16. Y. Chen, G. Lin and S. Chen, *Langmuir*, 2020, **36**, 7715–7723.
17. F. Liu, S. Chen and Y. Gao, *J. Colloid Interface Sci.*, 2017, **506**, 236–244.
18. Y. Liu, Q. Ye, M. Shen, J. Shi, J. Chen, H. Pan and Y. Shi, *Environ. Sci. Technol.*, 2011, **45**, 5710–5716.
19. R. A. Khatri, S. S. Chuang, Y. Soong and M. Gray, *Energy Fuels*, 2006, **20**, 1514–1520.
20. H. Li, H. Guo and S. Shen, *ACS Sustain. Chem. Eng.*, 2020, **8**, 12956–12967.
21. M. Tao, J. Gao, W. Zhang, Y. Li, Y. He and Y. Shi, *Ind. Eng. Chem. Res.*, 2018, **57**, 9305–9312.
22. N. J. Williams, C. A. Seipp, F. M. Brethomé, Y.-Z. Ma, A. S. Ivanov, V. S. Bryantsev, M. K. Kidder, H. J. Martin, E. Holguin, K. A. Garrabrant and R. Custelcean, *Chem*, 2019, **5**, 719–730.
23. R. Custelcean, N. J. Williams, K. A. Garrabrant, P. Agullo, F. M. Brethomé, H. J. Martin and M. K. Kidder, *Ind. Eng. Chem. Res.*, 2019, **58**, 23338–23346.
24. F. M. Brethomé, N. J. Williams, C. A. Seipp, M. K. Kidder and R. Custelcean, *Nature Energy*, 2018, **3**, 553–559.
25. H. Cai, X. Zhang, L. Lei and C. Xiao, *ACS Omega*, 2020, **5**, 20428–20437.
26. R. Custelcean, *Chem. Sci.*, 2021, **12**, 12518–12528.
27. F. Inagaki, C. Matsumoto, T. Iwata and C. Mukai, *J. Am. Chem. Soc.*, 2017, **139**, 4639–4642.
28. J. M. Hanusch, I. P. Kerschgens, F. Huber, M. Neuburger and K. Gademann, *Chem. Commun.*, 2019, **55**, 949–952.
29. A. I. Papadopoulos, F. Tzirakis, I. Tsivintzelis and P. Seferlis, *Ind. Eng. Chem. Res.*, 2019, **58**, 5088–5111.
30. H. Machida, R. Ando, T. Esaki, T. Yamaguchi, H. Horizoe, A. Kishimoto, K. Akiyama and M. Nishimura, *Int. J. Greenh. Gas Control.*, 2018, **75**, 1–7.

31. K. V. B. Tran, R. Ando, T. Yamaguchi, H. Machida and K. Norinaga, *Ind. Eng. Chem. Res.*, 2020, **59**, 3475–3484.
32. H. Yamada, *Polym. J.*, 2020, **53**, 93–102.
33. T.-a. Mitsudo, Y. Hori, Y. Yamakawa and Y. Watanabe, *Tetrahedron Lett.*, 1987, **28**, 4417–4418.
34. W. Buijs and S. de Flart, *Ind. Eng. Chem. Res.*, 2017, **56**, 12297–12304.
35. N. Noorani and A. Mehrdad, *Fluid Phase Equilib.*, 2020, **517**, 112591–112598.
36. A. a. F. Eftaiha, A. K. Qaroush, K. I. Assaf, F. Alsoubani, T. Markus Pehl, C. Troll and M. I. El-Barghouthi, *New J. Chem.*, 2017, **41**, 11941–11947.
37. P. D. Vaidya and E. Y. Kenig, *Chemical Engineering & Technology*, 2007, **30**, 1467–1474.
38. D. W. Keith, G. Holmes, D. St. Angelo and K. Heidel, *Joule*, 2018, **2**, 1573-1594.
39. V. S. Derevschikov, J. V. Veselovskaya, T. Y. Kardash, D. A. Trubitsyn and A. G. Okunev, *Fuel*, 2014, **127**, 212–218.
40. L. H. Ngu, J. W. Song, S. S. Hashim and D. E. Ong, *Greenhouse Gases: Science and Technology*, 2019, **9**, 519-528.
41. G. Holmes and D. W. Keith, *Philos Trans A Math Phys Eng Sci*, 2012, **370**, 4380-4403.
42. J. A. Wurzbacher, C. Gebald, N. Piatkowski and A. Steinfeld, *Environ Sci Technol*, 2012, **46**, 9191–9198.
43. X. Zhu, T. Ge, F. Yang and R. Wang, *Renew. Sust. Energ. Rev.*, 2021, **137**, 110651–110662.

Acknowledgement

This study is based on results obtained from a project, JPNP14004, subsidized by the New Energy and Industrial Technology Development Organization (NEDO).

Author contributions

S.K. and S.Y. designed this study. K.A. and Y.F. contributed to all experimental works and data analysis. S.K. and J.H. conducted experimental setup and data analysis. G.K., H.M. and T.S. characterized the carbamic acids. S.K. and S.Y. proposed the mechanism with the help of H.M. and T.S. S.Y. supervised this study. All authors took part in the writing of this manuscript.

Competing interests

The authors declare no competing interests.